Cell Motility and the Cytoskeleton 49:67–77 (2001)

Mutagenesis of β-Tubulin Cysteine Residues in *Saccharomyces cerevisiae:* Mutation of Cysteine 354 Results in Cold-Stable Microtubules

Mohan L. Gupta, Jr.,[1] Claudia J. Bode,[1] Cynthia A. Dougherty,[2] Rebecca T. Marquez,[3] and Richard H. Himes[1]*

[1]*Department of Molecular Biosciences, University of Kansas, Lawrence, Kansas*
[2]*Department of Biology, Johns Hopkins University, Baltimore, Maryland*
[3]*University of Texas, MD Anderson Cancer Center, Houston, Texas*

Cysteine residues play important roles in the control of tubulin function. To determine which of the six cysteine residues in β-tubulin are critical to tubulin function, we mutated the cysteines in *Saccharomyces cerevisiae* β-tubulin individually to alanine and serine residues. Of the twelve mutations, only three produced significant effects: C12S, C354A, and C354S. The C12S mutation was lethal in the haploid, but the C12A mutation had no observable phenotype. Based on interactive views of the electron crystallographic structure of tubulin, we suggest that substitution of serine for cysteine at this position has a destabilizing effect on the interaction of tubulin with the exchangeable GTP. The two C354 mutations, although not lethal, produced dramatic effects on microtubules and cellular processes that require microtubules. The C354 mutant cells had decreased growth rates, a slowed mitosis, increased resistance to benomyl, and impaired nuclear migration and spindle assembly. The C354A mutation produced a more severe phenotype than the C354S mutation: the haploid cells had chromosome segregation defects, only 50% of cells in a culture were viable, and a significant percentage of the cells were misshapened. Cytoplasmic microtubules in the C354S and C354A cells were longer than in the control strain and spindle structures appeared shorter and thicker. Both cytoplasmic and spindle microtubules in the two C354 mutants were extremely stable to cold temperature. After 24 h at 4°C, the microtubules were still present and, in fact, very long and thick tubulin polymers had formed. Evidence exists to indicate that the C354 residue in mammalian tubulin is near the colchicine binding site and the electron crystal structure of tubulin places the residue at the interface between the α- and β-subunits. The sulfhydryl group is situated in a polar environment, which may explain why the alanine mutation is more severe than the serine mutation. When the C12S and the two C354 mutations were made in a diploid strain, the mutated tubulin was incorporated into microtubules and the resulting heterozygotes had phenotypes that were intermediate between those of the mutated haploids and the wild-type strains. The results suggest that the C12 and C354 residues play important roles in the structure and function of tubulin. Cell Motil. Cytoskeleton 49:67–77, 2001.

Key words: cold-stable microtubules; yeast tubulin; tubulin cysteines; in vitro mutagenesis

Abbreviations used: DMSO, dimethylsulfoxide; EGTA, ethylene glycol bis(β-aminoethylether)-N,N,N′,N′-tetraacetic acid; PEM, 0.1 M Pipes, 1 mM EGTA, 1 mM $MgSO_4$, pH 6.9; Pipes, 1,4-piperazinediethanesulfonate.

Contract grant sponsor: National Institutes of Health; Contract grant number: CA55141; Contract grant sponsor: University of Kansas.
*Correspondence to: Richard H. Himes, Department of Molecular Biosciences, University of Kansas, Lawrence, KS 66045-2106. E-mail: himes@ukans.edu

Received 7 December 2000; Accepted 21 March 2001

INTRODUCTION

Microtubules participate in essential cellular processes, including intracellular transport and chromosome movement and segregation during mitosis and meiosis. The protein subunit of microtubules, tubulin, is a heterodimer consisting of α- and β-monomers, which are about 45% identical in amino acid sequence. Each monomer contains a tightly bound GTP. In spite of the essential nature of tubulin in eukaryotic cells, many structural and functional properties of the protein are not understood.

A number of in vitro studies have shown that modifications of cysteine residues alter the biochemical properties of tubulin. For example, alkylation or oxidation of just a few of the 20 cysteine residues in mammalian brain tubulin leads to complete inhibition of tubulin assembly in vitro [reviewed by Ludueña and Roach, 1991]. In fact, it has been proposed that the reversible formation of disulfides may be an important type of physiological control of microtubule formation [Khan and Ludueña, 1991]. Evidence has also been presented that suggests a cysteine residue is involved in the catalysis of GTP hydrolysis in the intrinsic GTPase activity of tubulin [Mejillano et al., 1996]. Specific cysteine residues in mammalian brain β-tubulin have been shown to interact with ligands or be involved in tubulin function. Upon uv-induced crosslinking, the exchangeable nucleotide in the β-subunit becomes covalently bound to β-C12 [Shivanna et al., 1993; Jayaram and Haley, 1994] and β-C211 [Bai et al., 1999]. β-C12 can be crosslinked to β-C201 or β-C211 by a bifunctional sulfhydryl reagent if the nucleotide is removed from the E-site [Little and Ludueña, 1987]. β-C354 has been shown to react covalently with an analogue of colchicine [Bai et al., 1996] and apparently is the cysteine that is modified by pyrene-maleimide [Basusarkar et al., 1997]. This residue can also be crosslinked to β-C239 [Little and Ludueña, 1985]. β-C239 has also been associated with the loss of assembly activity when tubulin is modified with the anti-mitotic agent 2,4-dichlorobenzyl thiocyanate [Bai et al., 1989] and is selectively modified by the anti-mitotic compound 2-fluoro-1-methoxy-4-pentafluorophenylsulfonamido-benzene [Shan et al., 1999]. Evidence has also been presented to show that this residue is modified by low molar ratios of N-ethyl maleimide leading to a modified tubulin that preferentially inhibits assembly at the minus end of the microtubule [Phelps and Walker, 2000]. Thus, it is apparent that cysteine residues in the β-subunit play important roles in the structure and activity of tubulin.

We have undertaken an investigation of the role of the β-tubulin cysteine residues with the use of in vitro site-directed mutagenesis in budding yeast. *Saccharomyces cerevisiae* tubulin contains 17 cysteine residues, 11 in α-tubulin, and 6 in β-tubulin. It is an excellent organism to use in such studies because it contains only one β-tubulin gene, *TUB2* [Neff et al., 1983]. We plan to examine the consequences of individual β-tubulin cysteine mutations on microtubule-related processes at the cellular level and on tubulin properties in vitro. This report specifically focuses on the phenotypic effects of mutating all six β-tubulin cysteine residues, C12, C25, C127, C201, C211, and C354, individually to alanine and serine residues. As described above, in vitro studies with mammalian tubulin provide evidence that the C12, C201, C211, and C354 residues may be important in the structure and function of tubulin. The results demonstrate that β-tubulin mutations affecting C25, C127, C201, or C211, have little or no effect on microtubule-related processes. The only observed phenotype was an increased sensitivity to the anti-mitotic compound benomyl in the C25S, C25A, C201S, C201A, and C211A mutants. The C12A mutant behaves as the control strain while the C12S mutation is lethal. The C354S and C354A mutations affect both cytoplasmic and spindle microtubule functions and result in the formation of extremely cold-stable microtubules. In fact, microtubules in these C354 mutants appear to be completely stable to low temperature. Our results suggest that the highly conserved cysteine residues C12 and C354 play roles in tubulin function in vivo.

MATERIALS AND METHODS

DNA Manipulations

TUB2 plasmids originated from pCS3, which has a 5,000-bp SacI/SphI fragment containing *TUB2* along with 1,165-bp of flanking genomic sequence upstream, 1,370-bp downstream, and *URA3* cloned 985-bp downstream from the *TUB2* open-reading frame [Sage et al., 1995]. pMG1 was created from pCS3 using oligonucleotide-directed mutagenesis (Stratagene QuikChange) to introduce a His_6 tag $(CAC)_6$ just before the *TUB2* stop codon. The His_6 tag was added to facilitate purification of tubulin from the mutants. Site-directed mutagenesis of cysteine-coding sequences in *TUB2* was performed in pMG1 using oligonucleotide-mediated mutagenesis. The targeted cysteine residues were mutated to GCT or TCT for Ala and Ser substitutions, respectively, based on the preferred codons in yeast [Hinnebusch and Liebman, 1991]. All mutations were verified by DNA sequencing on a Li-Cor 4000L automated sequencer operated by the Biochemical Research Services Laboratory at the University of Kansas.

Strains and Media

The haploid strains used in this study were derived from the strain FY41 (genotype: *MATa, leu2, ura3, his4, trp1*) [Schatz et al., 1986]. MGY1 was constructed by transformation of FY41 with the gel-purified SacI/SphI fragment of pMG1 using the lithium acetate method of Ito et al. [Ito et al., 1983] and selecting for colonies on media lacking uracil. MGY1 strains containing *TUB2* cysteine mutations were created the same way using mutated pMG1. The diploid strain used was strain MAY1210 (genotype: *MATa/MATα, ADE2/ade2, his3/his3, leu2/leu2, LYS2/lys2, ura3/ura3*) [Hoyt et al., 1991].

Mutations were verified by DNA sequencing. Yeast genomic DNA was prepared by the method of Cryer et al. [1975]. The primer pair 5′-GTGAGGCAATTGGAGTGACATAGCAGC-3′ (upstream) and 5′-GCTCCAAGTGCTTCAATCCTAGAGAAGAAGAAAGG-3′ (downstream) was used to amplify genomic *TUB2* by PCR.

Yeast strains were routinely grown in YPD medium (1% yeast extract, 2% peptone, and 2% glucose) at 30°C. Yeast transformants were selected for conversion to prototrophy by growth in SD medium (0.67% yeast nitrogen base without amino acids and 2% glucose) supplemented with the appropriate metabolites. *Escherichia coli* strain XL1-Blue (Stratagene) was grown at 37°C in LB medium (1% bactotryptone, 0.5% yeast extract, 1% NaCl) with 50 μg/mL ampicillin to select for inclusion of plasmids. Plasmids were purified using the Qiagen QIAquick kit.

Growth Rate and Benomyl Sensitivity

To determine growth rates, cultures grown overnight were inoculated into YPD medium to give an optical density at 600 nm of 0.05 and cultures were incubated at 15, 30, or 37°C with shaking at 225 rpm. Generation times were calculated from the increase in optical density over a minimum of four doublings. In the case of mutant strains with increased cell size, the growth rates were verified by manual cell counts using a haemocytometer. Benomyl sensitivity was determined by spreading cultures onto YPD plates containing this antimitotic drug followed by incubation at 30°C for 3 to 5 days. Plates were prepared by diluting a 10 mg/mL stock solution of benomyl in DMSO in warm media to a final benomyl concentration range of 5–85 μg/mL. Control plates were prepared by adding equivalent volumes of DMSO to warm media. Benomyl sensitivity is defined as the lowest concentration of benomyl that completely inhibited growth.

Cell Size and Viability

The cell size distribution of exponentially growing yeast cultures was measured using a CASY 1 Cell Counter and Analyzer (Schärfe System). At least 10,000 cells were analyzed per experiment to determine the average cell diameter. To determine viability, exponentially growing cultures were diluted, counted, and about 100 cells from these cultures were spread onto YPD plates at 30°C. Cell viability was scored by colony formation after incubation for 3 days at 30°C.

Bud Morphology, Nuclear Position, and Microtubule Lengths

To visualize microtubules by immunofluorescence microscopy, exponentially growing cultures were fixed and stained using the method of Pringle and Hartwell [1981]. The primary antibody was the anti-α-tubulin antibody YOL 1/34 [Kilmartin et al., 1982]. The secondary antibody was a fluorescein-conjugated goat anti-rat antibody. Both antibodies were purchased from Accurate Chemical and Scientific Corp. and were used at a 1:250 dilution. To confirm the incorporation of mutated tubulin in microtubules in heterozygous diploids, the primary antibody was the anti-His_6 monoclonal antibody (Tetra-His, Qiagen) used at a 1:100 dilution and the secondary antibody was the fluorescein-conjugated goat anti-mouse antibody (Accurate Chemical and Scientific Corp.) used at a 1:50 dilution. Cells were visualized on a Zeiss Axiophot epifluorescence microscope using either a 63×/1.25NA or 100×/1.3NA objective. A Hamamatsu SIT-video camera linked to the Metamorph image processing system (Universal Imaging) was used to capture images.

An abbreviated version of the method of Pringle et al. [1991] was used to prepare exponentially growing cultures for visualization of bud morphology and nuclear position. After fixation, cells were adhered to slides, blocked, and stained with Hoechst 33342 (1 μg/mL). Using a combination of epifluorescence and phase-contrast microscopy, cells were classified as unbudded, small-budded, or large-budded (>50% of mother cell diameter). Large-budded cells were further classified as having the nucleus in the mother cell, at the bud neck, or segregated into the mother and daughter cells. The cell morphology of mutant cultures was determined by viewing the cells using differential-interference-contrast microscopy.

To determine microtubule lengths, immunofluorescence images were acquired from three separate cultures and cytoplasmic microtubules were measured from the edge of spindle pole body fluorescence to the end of the microtubule using NIH Image version 1.61.

Flow Cytometry of Yeast Cultures

Asynchronous log-phase cultures were fixed and stained with propidium iodide using a procedure based on one described by Hutter and Eipel [1978]. Flow

cytometry was performed on a Becton Dickinson FACScan and analyzed using the Cell Quest software. For each experiment at least 10,000 cells were analyzed.

Tetrad Analysis

Diploid strains were sporulated on solid sporulation media (1% potassium acetate, 0.1% yeast extract, 0.05% dextrose, and 2% agar) and tetrads were dissected by standard methods [Sherman and Hicks, 1991]. Segregation of metabolic markers was assessed by growth of the individual spores on appropriate drop-out media and mating-type was determined by the ability to complement *MATa, ade6,* and *MATα, ade6* strains.

RESULTS

To determine whether the cysteine residues in β-tubulin are essential for microtubule function and thus for cell viability, we introduced each of the cysteine to alanine and serine substitutions individually into the wild-type diploid strain MAY1210 creating *tub2/TUB2* heterozygous diploid strains. Each of these diploid strains was sporulated and the viability of the haploids from the resulting tetrads was assessed. All four spores generated by the diploid strains containing the *tub2*-C25, -C127, -C201, or -C211 alanine or serine mutations were viable. The four spores from tetrads generated by the diploid strain containing the *tub2*-C12A mutation were also viable, but tetrads from the *tub2*-C12S/*TUB2* strain produced only two viable spores. None of the viable spores from this strain were Ura^+ and since the *URA3* gene is tightly linked to *tub2*-C12S, we conclude that C12S is a lethal mutation. The lethality was verified in a second, independent transformant. There was also a difference between the spore viability in tetrads generated from the *tub2*-C354S/*TUB2* and *tub2*-C354A/*TUB2* strains. While the four spores from the *tub2*-C354S/*TUB2* tetrads were viable, tetrads from *tub2*-C354A/*TUB2* showed variable spore viability, between two to four surviving daughters. The *tub2*-C354A spores germinated at a reduced efficiency and grew at much slower rates than their *TUB2* sisters.

The non-lethal cysteine to alanine and serine substitutions were made directly in the haploid strain MGY1 (*tub2*-His_6) and all mutant strains were assayed for growth rate, cell size, benomyl sensitivity, bud morphology, nuclear migration, and DNA content. With the exception of C354A and C354S, all other mutants exhibited either no or small phenotypic changes when compared to MGY1 (Table I). C12A, C211S, and both of the C127 mutants had phenotypes indistinguishable from the MGY1 phenotype. The C25A, C25S, C201A, C201S, and C211A mutants exhibited increased sensitivity to benomyl. The most pronounced phenotypes, however, were observed in the C354S and C354A mutants, which are the focus of this report.

TABLE I. Phenotypes of β-Tubulin Cysteine Mutants

Mutation	Phenotype
C12A	Wild-type
C12S	Recessive lethal
C25A	Benomyl supersensitive
C25S	Benomyl supersensitive
C127A	Wild-type
C127S	Wild-type
C201A	Benomyl supersensitive
C201S	Benomyl supersensitive
C211A	Benomyl supersensitive
C211S	Wild-type
C354A	Benomyl resistant, slow growth at 15, 30, and 37°C; mitotic slowdown, cold-stable MTs, abnormal morphology
C354S	Benomyl resistant, slow growth at 15 and 37°C; mitotic slowdown, cold-stable MTs

In Figure 1, the doubling times, benomyl sensitivity, and cell size of the C354S and C354A mutants are compared to those of the control strain MGY1. The doubling time of the C354A mutant at 30°C was 73% higher than that for MGY1, but the growth rate of C354S was not affected at this temperature (Fig. 1A). At 15 and 37°C, both mutants grew slower than MGY1. In the case of C354A, the doubling time was 324% higher at 15°C. Both mutants showed a significant increase in resistance to the anti-mitotic compound benomyl (Fig. 1B) and both were larger in size than the control strain (Fig. 1C). The size increase was especially apparent in the alanine mutant, which had a 160% greater mean diameter than MGY1 at 30°C. The increase in size was also found at 15 and 37°C.

The increase in cell size of the C354A mutant was also observed by DIC-microscopy (Fig. 2). Not only were the mutant cells clearly larger than MGY1 cells, but cells with abnormal shapes were evident in cultures of this mutant as well as the C354S mutant (data not shown). About 25% of the cells of the C354A cultures contained elongated buds, elongated necks, what appeared to be chains of buds, and otherwise misshapen appearances (Fig. 2).

Cell viability of both of the C354 mutants was measured. Exponentially growing cells were diluted and counted in a haemocytometer. A known number of cells was used to inoculate agar plates and colony formation was scored. MGY1 and C354S were 100% viable. However, only 44% of the cells in a culture of the C354A mutant were viable.

FACS analyses were performed to determine the DNA content distribution of asynchronously grown log-phase cultures. Cultures of haploid cells containing a

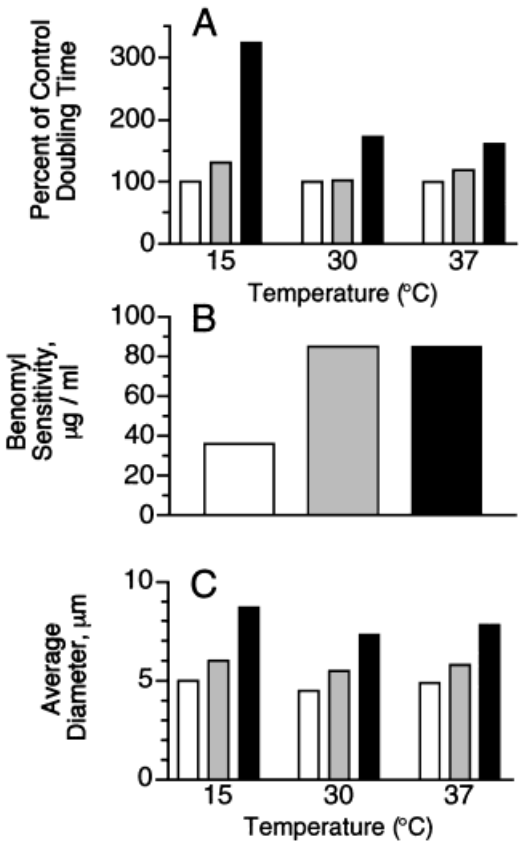

Fig. 1. Effects of the C354 mutations on cell growth and benomyl sensitivity. Details of the experiments are presented in Materials and Methods. *Open bars*, MGY1. *Gray bars*, C354S. *Black bars*, C354A. **A:** Doubling times. The doubling time for the control strain MGY1 was 412 min at 15°C, 134 min at 30°C, and 157 min at 37°C. The results represent the means of 2 to 3 experiments. **B:** Benomyl sensitivity. The concentration of benomyl that completely inhibited growth for each strain. **C:** Mean diameters of log-phase cells.

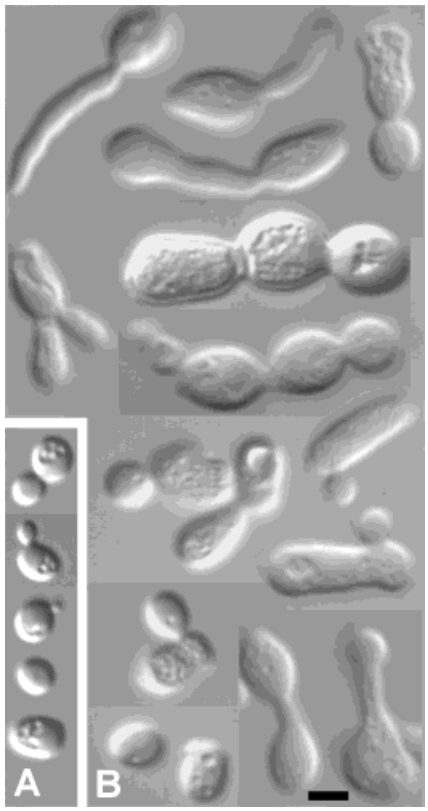

Fig. 2. DIC images of MGY1 and C354A mutant cells. **A:** MGY1. **B:** Representative views of misshapened C354A cells. Approximately 25% of the cells in a culture had misshapened morphologies. Bar = 5 µm and applies to A and B.

mutation that slows mitosis would be expected to show an increase in the proportion of cells with a 2N DNA content. This was the case for the C354S mutant (Fig. 3). The control culture, MGY1, contained an equal distribution between 1N and 2N cells while the C354S culture had a 50% increase in 2N cells. On the other hand, the C354A culture contained a large percentage of 2N cells and a broad distribution of cells with a higher DNA content.

It is apparent from the decreased growth rate and the increased percentage of cells with 2N DNA content that these tubulin mutations affect timely progression through the cell cycle. Quantification of bud morphology provides information about cell-cycle kinetics. Unbudded cells are in G1 phase, cells with small buds are in S phase approaching G2, and large-budded cells are in G2/M [Pringle and Hartwell, 1981]. Figure 4A contains the results of this analysis for the two C354 mutants. Only cells containing one bud and normal morphology

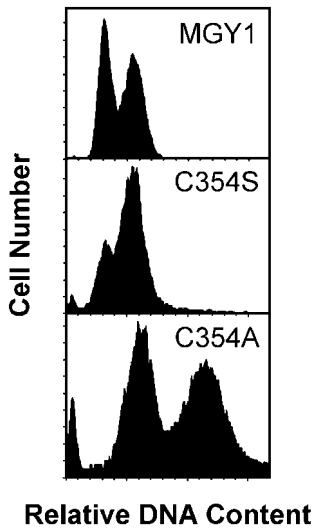

Fig. 3. FACS analysis of MGY1 and the C354 mutants. Log phase cells were stained with propidium iodide and analyzed by flow cytometry.

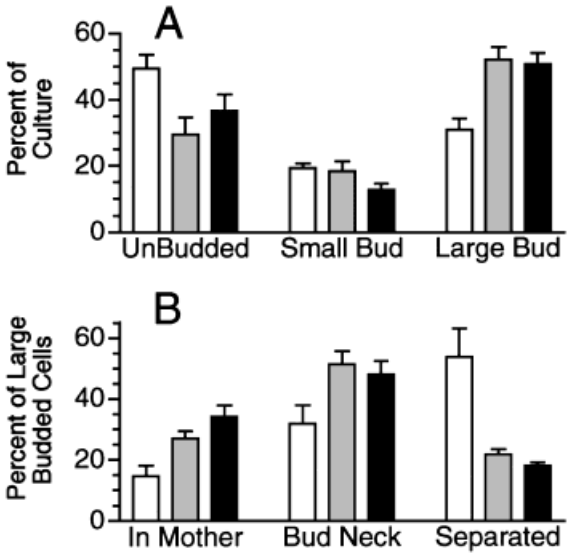

Fig. 4. Bud morphology and nuclear position. **A:** Phase-contrast images were used to determine the number of cells with no bud, a small bud, or a large bud. The data represent the means of three experiments and the error bars represent standard deviations. In each experiment, 400 cells were observed. **B:** Cells were stained with Hoechst 33342 stain as described in Materials and Methods and the position of the nucleus in large-budded cells was determined. *Open bar*, MGY1. *Gray bar*, C354S. *Black bar*, C354A.

were included in the analysis. When compared to MGY1, exponentially growing cultures of both of the C354 mutants showed a higher proportion of large-budded cells and a smaller proportion of unbudded cells, suggesting a slowdown in mitosis.

Microtubules in budding yeast function in positioning the nucleus at the neck of the budding cell prior to chromosome segregation and in separating the chromosomes [Huffaker et al., 1988]. During the G2/M transition of the cell cycle, the nucleus normally migrates rapidly to the bud neck of large-budded cells. At the onset of anaphase, the chromosomes are then segregated into the two daughter cells. By quantifying the position of the nucleus in large-budded cells, whether in the mother cell, at the bud neck, or separated into the mother cell and the bud, it is possible to identify defects in the microtubule-dependent processes of nuclear migration and chromosome segregation. In the two C354 mutants, there was a significant decrease in the percentage of large-budded cells with separated nuclei and a corresponding increase in cells with the nuclei positioned at the neck or in the mother cell (Fig. 4B). This suggests that both nuclear migration and chromosome separation are substantially slowed in these mutants.

Elongated spindles are found in large-budded cells that are proceeding through anaphase. If the two C354 mutants have problems in elongating the mitotic spindle, a decrease in the percentage of large-budded cells that

TABLE II. Mitotic Cells With Elongated Spindles*

Strain	Cells in culture with spindle (%)	Large-budded cells in culture (%)	Large-budded cells with spindles (%)
MGY1	8.5	31	27.3
C354S	3.4	52	6.5
C354A	4.1	51	8.1

*The results represent the examination of between 1,500 and 2,300 cells. Only elongated spindles were counted.

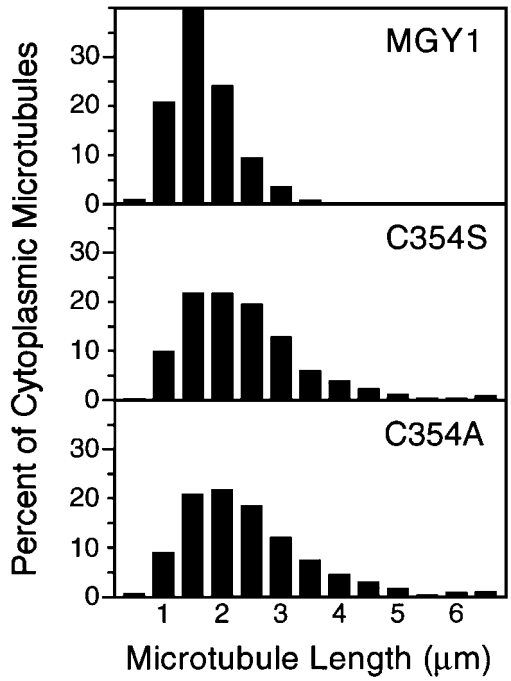

Fig. 5. Length distribution of cytoplasmic microtubules. Cells were stained with an α-tubulin antibody and microtubules were visualized by fluorescence microscopy. The lengths of cytoplasmic microtubules were determined as described in Materials and Methods. Approximately 1,000 microtubules in each strain were measured.

contain elongated spindles would occur. Indirect immunofluorescence was used to determine the number of elongated spindles in a population of large-budded cells and the results are presented in Table II. From the data in Table II, it is clear that there is a large decrease in the percentage of mitotic cells that contain elongated spindles in both C354 mutants. The spindles in the two C354 mutants also appeared thicker.

Since microtubule-dependent processes are affected in the C354 mutants, we determined whether the microtubules themselves were also altered. We measured the mean microtubule lengths of cytoplasmic microtubules in asynchronous cultures at 30°C as visualized by indirect immunofluorescence (Fig. 5). The length distributions show a shift towards longer cytoplasmic microtubules in the two mutant strains. The mean lengths were 1.44, 2.09, and 2.18 μM for MGY1, C354S, and C354A,

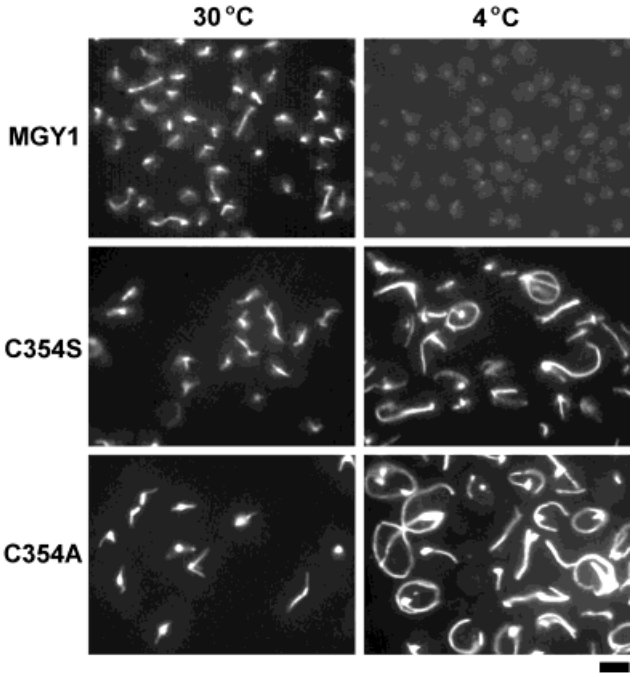

Fig. 6. Cold stability of microtubules in MGY1 and C354 mutants. Log-phase cells were incubated at 4°C for 24 h, stained with an α-tubulin antibody, and microtubules were visualized by fluorescence microscopy. Bar = 5 μm.

respectively ($P < 0.001$). The mean length for MGY1 microtubules is similar to the length reported for another *S. cerevisiae* strain [Tirnauer et al., 1999]. The differences between microtubule lengths in the C354 mutants compared to MGY1 cells may actually be underestimated as cells in G1 have longer cytoplasmic microtubules on average than cells in mitosis [Huffaker et al., 1988] and the C354 mutant cultures have a smaller percentage of G1 cells.

The results we have presented thus far suggest that mutation of cysteine 354 to an alanine or serine residue affects the ability of microtubules to function in nuclear migration and mitosis. Such an effect could result from a change in microtubule stability. We tested this hypothesis by examining the cold stability of the cellular microtubules since microtubules are generally cold-labile. Cells were incubated at 4°C and examined by tubulin indirect immunofluorescence (Fig. 6). In MGY1 cells, cytoplasmic microtubules had disappeared after 2 hr but some spindle microtubules were still present (data not shown). After 6 h, the spindle microtubules were gone and small dots of fluorescence were present, presumably at the spindle pole body [Huffaker et al., 1988]. These dots did disappear after 24 h. On the other hand, microtubules in the two C354 mutants were clearly more stable than those in MGY1, as they persisted even after 24 h at 4°C. In fact, after this period the cytoplasmic microtubules in the C354 mutants were much longer than those at 30°C and were arranged in unusual patterns (Fig. 6). These tubulin polymers resembled individual microtubules, but could possibly be bundles of microtubules or other polymeric structures. In some cases, the microtubules or tubulin polymers extended from the spindle pole body around the cortex of the cells and buds. Although the microtubules in the C354S and C354A strains were extremely cold-stable, they could be depolymerized at 4°C if benomyl was added to the medium. When cells were treated for 24 h in the cold and then returned to 30°C, the microtubules assumed the appearance they had before being placed in the cold (data not shown).

To assess the possible influence of the His_6 tag on the results, we made the C354 mutations in the FY41 strain and compared selected phenotypes of these mutants to the mutants made in MGY1. The phenotypes of the parent strains FY41 and MGY1 were indistinguishable. In addition, the FY41-C354 mutants exhibited the same phenotypes as those made in MGY1, indicating that the His_6 tag on β-tubulin did not contribute to the results. This is not surprising since it is known that the last 12 amino acids in the C-terminus of yeast β-tubulin can be removed without a noticeable effect on the phenotype [Katz and Solomon, 1988].

In addition, we analyzed the C354A and C354S haploid strains that were obtained from tetrad dissections of the mutant heterozygous diploid strains. These haploids had the same characteristics (cold-stable microtubules, decreased benomyl sensitivity, abnormal DNA content) as the strains derived from the MGY1 mutations. These data demonstrate that the cellular phenotypes observed in the MGY1-C354 mutants were a direct result of the C354 mutations and not of a secondary mutation.

We also examined the phenotypes of the heterozygous diploid strains containing the C12S, C354A, and C354S mutations. Although the C12S mutation was lethal in the haploid, in the *tub2*-C12S/*TUB2* diploid strain the mutated protein was incorporated into microtubules as observed by anti-His_6 immunostaining. In addition, the diploid strain grew slower at 30 and 37°C and was delayed in mitosis as shown by characteristics of a slow-down in mitosis (increased 4N DNA content, increased percentage of large-budded cells with nuclei in the mother cell, and decreased percentage of large-budded cells with segregated nuclei). The unusual cold-stable microtubule phenotype of the C354S and C354A haploid strains was also observed in the heterozygous *tub2*-C354S/*TUB2* and *tub2*-C354A/*TUB2* diploid strains. The incorporation of the mutated proteins into cellular microtubules was demonstrated with an anti-His_6 antibody. After incubation of the cells for 24 h at 4°C, microtubules were still present (Fig. 7). However, in contrast to the

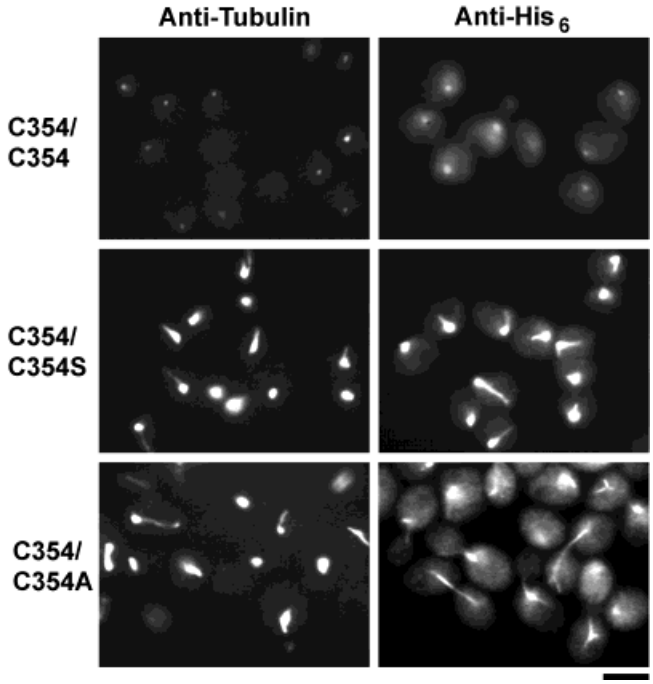

Fig. 7. Cold stability of microtubules in the diploid strains MAY1210-His_6, *tub2*-C354A/*TUB2*, and *tub2*-C354S/*TUB2*. Log-phase cells were incubated at 4°C for 24 h, stained with α-tubulin and His_6 antibodies, and visualized by fluorescence microscopy. Bar = 5 μm.

microtubules in the haploid mutant strains, they did not appear to continue to grow at this temperature. In addition to the presence of cold-stable microtubules, the heterozygous diploid strains *tub2*-C354A/*TUB2* and *tub2*-C354S/*TUB2* were also more resistant to benomyl than the control strain (45 μg/mL for the mutant strains vs. 15 μg/mL for the control strain). FACS analysis showed that both C354 mutant diploid strains had a normal DNA content distribution.

DISCUSSION

Various types of in vitro biochemical studies have demonstrated that cysteine residues play important roles in the properties of tubulin. *S. cerevisiae* tubulin contains 17 cysteine residues, 11 in the α-subunit and 6 in the β-subunit. In each subunit, some of the cysteines are very highly conserved. To determine which of the cysteines in the β-subunit are important to the biological function of tubulin, we mutated the six residues individually to alanine and serine residues. Tetrad analysis demonstrated that the only lethal mutation was C12S. Because haploid strains with mutations that changed residues C25, C127, C201, and C211 showed no dramatic change in phenotype, we conclude that these four cysteine residues have little or no role in microtubule cellular function. Based on the electron crystal structure of tubulin, C25 is located in the N-terminal region of the loop between helix 1 and β strand 2 [Nogales et al., 1998]. It is not surprising that the C25 mutations had little effect since in most β-tubulin sequences the residue at this position is alanine. C127 is located in a small loop between helix 3 and β strand 4 [Nogales et al., 1998]. This loop is proposed to be involved in intra-dimer longitudinal contacts in the protofilament [Nogales et al., 1999]. C201 and C211 are located near the ends of β strand 6 and helix 6, respectively [Nogales et al., 1998]. Helix 6 is proposed to make lateral contacts between adjacent protofilaments [Nogales et al., 1999]. Apparently the thiol group of each of these four cysteine residues is not critical to interactions within the microtubule.

Although the C12S mutation was lethal, the C12A mutation was not. In fact, the C12A mutant had no observable phenotype. C12 is situated at the start of helix 1 in the β-tubulin structure and interacts with the purine ring of the exchangeable nucleotide [Nogales et al., 1999]. Richards et al. [2000] have modeled the *S. cerevisiae* tubulin dimer containing Tub1p and Tub2p using the coordinates from the bovine brain tubulin structure. Interactive views of the model show that the thiol group of C12 is situated directly over the purine ring (Fig. 8). The sulfur atom of C12 is 3.6 and 4.3 Å, respectively, from C7 and C9 of the purine ring. Perhaps the more polar hydroxymethyl group of serine at this position alters GTP binding and/or hydrolysis. Consistent with this conclusion, all 179 published β-tubulin sequences contain a cysteine residue at position 12 (R. G. Burns, personal communication).

Mutation of C354, although not lethal, resulted in major changes in microtubule-related processes and microtubule stability. Log-phase cultures of the C354S and C354A haploid mutants at 30°C had a higher percentage of large-budded cells than log-phase cultures of the control strain MGY1, indicative of a slowdown during mitosis. In addition, a higher percentage of the large-budded cells contained the nucleus in the mother cell and at the neck when compared to MGY1. It is apparent that nuclear migration and chromosome segregation were affected in these mutants. Thus, both cytoplasmic and spindle microtubule functions were affected. Consistent with these results was the increase in the number of cells having a DNA content greater than 1N. In the C354S mutant, this was indicated by an increase in the population of 2N cells. However, cultures of the C354A mutant had very few cells with a 1N DNA content. Most of the cells had either a 2N or greater DNA content. The aneuploid nature of the C354A strain undoubtedly is related to the fact that only about 50% of cells in cultures of this mutant were viable and probably explains the large size of these cells [Galitski et al., 1999]. The decrease in

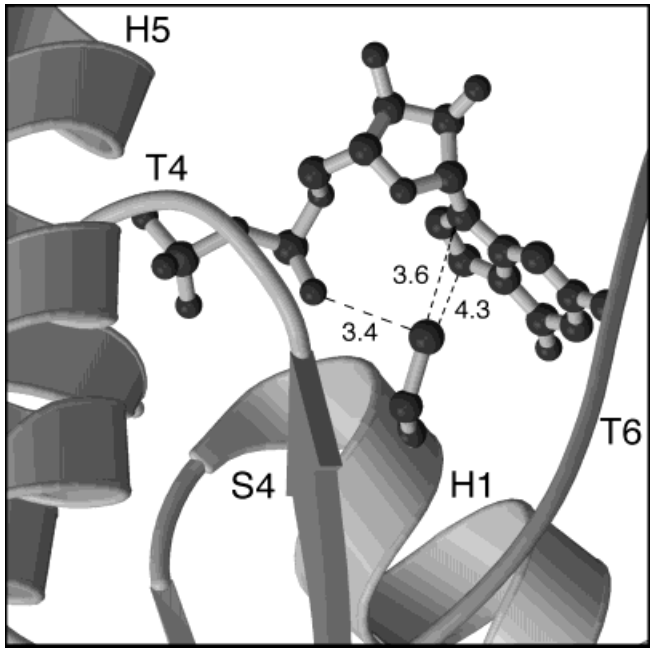

Fig. 8. Position of the C12 sulfur atom relative to the E-site nucleotide in Tub2p. The coordinates from the yeast tubulin model developed by Richards et al. [2000] were used to draw the structure. Helices H1 and H5, β strand 4, and loops T4 and T6 are shown. The LOOK software package (Molecular Applications Group, Palo Alto, CA) was used to obtain the distances between the sulfur atom and the purine ring and the α-phosphoryl oxygen. The distances are shown in angstroms. Prepared with MOLSCRIPT [Kraulis, 1991] and RASTER3D [Merrit and Murphy, 1994].

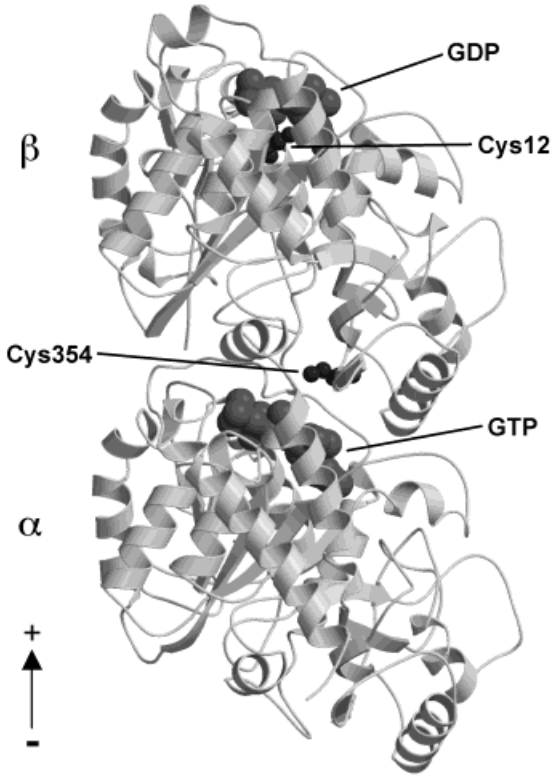

Fig. 9. Positions of C12 and C354 in β-tubulin. C12 is located near GDP in the E-site of β-tubulin and C354 is located at the interface between the α- and β-subunits. The figure shows the position of GDP in the E-site of β-tubulin and GTP in the N-site of α-tubulin. The view is from the outside of the microtubule. The + and − designations refer to the orientation of the microtubule. The structure was drawn using MOLSCRIPT [Kraulis, 1991] and RASTER3D [Merrit and Murphy, 1994].

viability also explains why tetrads from the *tub2*-C354A/*TUB2* diploid strain showed varied spore viability. Slow growth, large-sized cells, and cells with unusual morphology were also observed when the C354 mutations were introduced into a haploid strain that lacked the His_6 tag on β-tubulin (FY41). Therefore, we can conclude that these phenotypes are not the result of interactions between the His_6 tag and the C354 mutation.

The observed effects of the C354 mutations on microtubule-associated processes could be a result of an alteration in microtubule stability, since the dynamic nature of microtubules is critical to their function. Either an increase or decrease in stability would be expected to affect such events as nuclear migration and chromosome segregation. We found that replacement of the cysteine residue at position 354 in β-tubulin by serine or alanine greatly increased the stability of both the cytoplasmic and spindle microtubules, as indicated by the increased benomyl resistance and the extreme cold-stable nature of the microtubules. This drastic change in stability could be a result of changes in the strength of non-covalent lateral or longitudinal interactions between dimers in the microtubule, possibly lowering the critical protein concentration for assembly and decreasing microtubule dynamics. The C354 residue is located at the end of β strand 9, a strand that, in the α-subunit, is involved in inter-dimer longitudinal contacts within a protofilament but, in the β-subunit, is involved in intra-dimer contacts [Nogales et al., 1999] (Fig. 9). Using the LOOK software (Molecular Applications Group, Palo Alto, CA) we determined that the sulfur atom of β-C354 is surrounded by residues in the loop between helicies 7 and 8 and does not appear to be exposed to solvent, which is consistent with the report of Roychowdhury et al. [2000]. In addition, the sulfhydryl group is in a polar environment, consistent with the fact that the alanine mutation produced a more severe phenotype than the serine mutation. Although β strand 9 in β-tubulin is not involved in inter-dimer contacts, we propose that the mutations at C354 affect interactions within or between protofilaments. These mutations could result in conformational changes that affect longitudinal or lateral interactions. The evidence that the C354 residue is part of the colchicine-binding site [Bai et al., 1996; Roach and Ludueña, 1984], and binding of colchicine induces a conformational change in tubulin

[Hastie, 1991], provides support for the suggestion that a mutation at the 354 site could change the conformation of the protein. Additional evidence in support of the importance of this region of β-tubulin in controlling microtubule stability comes from studies with *Chlamydomonas* tubulin in which it was shown that mutation of K350 in β-tubulin caused resistance to colchicine [Lee and Huang, 1990].

A number of tubulin mutations in yeast are known to destabilize microtubules; however, as far as we are aware, the C354 mutations described in this report are the first shown to profoundly increase microtubule stability. However, a change in the residue at position 354 in β-tubulin is not the only change that can lead to cold-stability. For example, tubulins from cold-adapted fish brains, which contain cold-stable microtubules, have a cysteine residue at β-354 but contain several other amino acid substitutions that are probably responsible for increased microtubule stability [Modig et al., 1999; Detrich et al., 2000].

When the haploid-lethal C12S and both C354 mutations were introduced into a diploid strain, the resulting heterozygotes displayed phenotypes that appeared to be intermediate between the wild-type and mutated haploid strains. In all three cases, anti-His_6 immunostaining showed that the mutated proteins were incorporated into microtubules. The *tub2*-C12S/*TUB2* strain showed characteristics that could be attributed to a slowdown in mitosis. In the diploid strains heterozygous for the C354 mutations, the microtubules were cold-stable; but, in contrast to the mutated haploid strain, the microtubules did not appear to continue to elongate at 4°C. On the other hand, FACS analysis showed that the DNA content distribution was normal in both mutants. These results indicate that wild-type tubulin is able to compensate somewhat for the defects caused by mutated tubulin.

Our analyses of the β-tubulin cysteine mutant phenotypes demonstrate that amino acid residues 12 and 354 in *S. cerevisiae* β-tubulin are situated at sites that are important to the structure and function of microtubules. Further insight into the influence that these sites have on tubulin function can be obtained by studying the dynamic properties of the mutated proteins in vitro using purified tubulin, as well as in vivo using GFP-tubulin fusion proteins. Such studies are now underway in our laboratory.

ACKNOWLEDGMENTS

We thank Dr. K. Farrell for the yeast strain FY41 and Dr. A. Hoyt for strain MAY1210.

REFERENCES

Bai R, Lin CM, Nguyen NY, Liu T-Y, Hamel E. 1989. Identification of the cysteine residue of β-tubulin alkylated by the antimitotic agent 2,4-dichlorobenzyl thiocyanate, facilitated by separation of the protein subunits of tubulin by hydrophobic column chromatography. Biochemistry 28:5606–5612.

Bai R, Pei X-Y, Boyé O, Getahun Z, Grover S, Bekisz J, Nguyen NY, Brossi A, Hamel, E. 1996. Identification of cysteine 354 of β-tubulin as part of the binding site for the A ring of colchicine. J Biol Chem 271:12639–12645.

Bai R, Ewell JB, Nguyen NY, Hamel E. 1999. Direct photoaffinity labeling of cysteine 211 or a nearby amino acid residue of β-tubulin by guanosine 5′- diphosphate bound in the exchangeable site. J Biol Chem 274:12710–12714.

Basusarkar P, Chandra S, Bhattacharyya B. 1997. The colchicine-binding and pyrene-excimer-formation activities of tubulin involve a common cysteine residue in the β-subunit. Eur J Biochem 244:378–383.

Cryer DR, Eccleshall R, Marmur J. 1975. Isolation of yeast DNA. Methods Cell Biol 12:39–44.

Detrich HW III, Parker SK, Williams RC Jr, Nogales E, Downing KH. 2000. Cold adaptation of microtubule assembly and dynamics. Structural interpretation of primary sequence changes present in the α-and β-tubulins of antarctic fishes. J Biol Chem 275: 37038–37047.

Galitski T, Saldanha AJ, Styles CA, Lander ES, Fink GR. 1999. Ploidy regulation of gene expression. Science 285:251–254.

Hastie SB. 1991. Interactions of colchicine with tubulin. Pharmacol Ther 51:377–401.

Hinnebusch AG, Liebman SW. 1991. Protein synthesis and translational control in *Saccharomyces cerevisiae.* In: Pringle JR, Broach JR, Jones EW, editors. The molecular biology of the yeast *Saccharomyces.* Genome dynamics, protein synthesis and energetics. New York: Cold Spring Harbor Laboratory Press, p 627–735.

Hoyt MA, Totis L, Roberts BT. 1991. *S. cerevisiae* genes required for cell cycle arrest in response to loss of microtubule function. Cell 66:507–517.

Huffaker TC, Thomas JH, Botstein D. 1988. Diverse effects of β-tubulin mutations on microtubule formation and function. J Cell Biol 106:1997–2010.

Hutter K-J, Eipel HE. 1978. Flow cytometric determinations of cellular substances in algae, bacteria, and yeasts. Antonie Van Leeuwenhoek 44:269–282.

Ito H, FukudaY, Murata K, Kimura A. 1983. Transformation of intact yeast cells treated with alkali cations. J Bacteriol 153:163–168.

Jayaram B, Haley BE. 1994. Identification of peptides within the base binding domains of the GTP- and ATP-specific binding sites of tubulin. J Biol Chem 269:3233–3242.

Katz WS, Solomon F. 1988. Diversity among β-tubulins: a carboxy-terminal domain of yeast β-tubulin is not essential in vivo. Mol Cell Biol 8:2730–2736.

Khan IA, Ludueña RF. 1991. Possible regulation of the in vitro assembly of bovine brain tubulin by the bovine thioredoxin system. Biochim. Biophys. Acta 1076:289–297.

Kilmartin JV, Wright B, Milstein C. 1982. Rat monoclonal antitubulin antibodies derived by using a new nonsecreting rat cell line. J Cell Biol 93:576–582.

Kraulis PJ. 1991. MOLSCRIPT: a program to produce both detailed and schematic plots of protein structures. J Appl Crystallogr 24:946–950.

Lee VD, Huang B. 1990. Missense mutations at lysine 350 in β2-tubulin confer altered sensitivity to microtubule inhibitors in *Chlamydomonas*. Plant Cell 2:1051–1057.

Little M, Ludueña RF. 1985. Structural difference between brain β_1- and β_2-tubulins: implications for microtubule assembly and colchicine binding. EMBO J 4:51–56.

Little M, Ludueña RF. 1987. Location of two cysteines in brain β_1-tubulin that can be cross-linked after removal of exchangeable GTP. Biochim Biophys Acta 912:28–33.

Ludueña RF, Roach MC. 1991. Tubulin sulfhydryl groups as probes and targets for antimitotic and antimicrotubule agents. Pharmacol Ther 49:133–152.

Mejillano MR, Shivanna BD, Himes RH. 1996. Studies on the nocodazole-induced GTPase activity of tubulin. Arch Biochem Biophys 336:130–138.

Merrit EA, Murphy MEP. 1994. Raster3D version 2.0: a program for photorealistic molecular graphics. Acta Crystallogr D 50:869–873.

Modig C, Olsson P-E, Barasoain I, de Ines C, Andreu JM, Roach MC, Ludueña RF, Wallin M. 1999. Identification of β_{III}- and β_{IV}-tubulin isotypes in cold-adapted microtubules from Atlantic cod (*Gadus morhua*): antibody mapping and DNA sequencing. Cell Motil Cytoskeleton 42:315–330.

Neff NF, Thomas JH, Grisafi P, Botstein D. 1983. Isolation of the β-tubulin gene from yeast and demonstration of its essential function in vivo. Cell 33:211–219.

Nogales E, Wolf SG, Downing KH. 1998. Structure of the αβ tubulin dimer by electron crystallography. Nature 391:199–203.

Nogales E, Whittaker M, Milligan RA, Downing KH. 1999. High-resolution model of the microtubule. Cell 96:79–88.

Phelps KK, Walker RA. 2000. NEM tubulin inhibits microtubule minus end assembly by a reversible capping mechanism. Biochemistry 39:3877–3885.

Pringle JR, Hartwell LH. 1981. The *Saccharomyces cerevisiae* cell cycle. In: Strathern JN, Jones EW, Broach JR, editors. The molecular biology of the yeast *Saccharomyces.* Life cycle and inheritance. New York: Cold Spring Harbor Laboratory Press, p 97–142.

Pringle JR, Adams AEM, Drubin DG, Haarer BK. 1991. Immunofluorescence methods for yeast. Methods Enzymol 194:565–602.

Richards KL, Anders KR, Nogales E, Schwartz K, Downing KH, Botstein D. 2000. Structure-function relationships in yeast tubulins. Mol Biol Cell 11:1887–1903.

Roach MC, Ludueña RF. 1984. Different effects of tubulin ligands on the intrachain cross-linking of β_1-tubulin. J Biol Chem 259: 12063–12071.

Roychowdhury M, Sarkar N, Manna T, Bhattacharyya S, Sakar T, BasuSarkar P, Roy S, Bhattacharyya B. 2000. Sulfhydryls of tubulin. A probe to detect conformational changes of tubulin. Eur J Biochem 267:3469–3476.

Sage CR, Davis AS, Dougherty CA, Sullivan K, Farrell KW. 1995. β-Tubulin mutation suppresses microtubule dynamics in vitro and slows mitosis in vivo. Cell Motil Cytoskeleton 30:285–300.

Schatz PJ, Pillus L, Grisafi P, Solomon F, Botstein D. 1986. Two functional α-tubulin genes of the yeast *Saccharomyces cerevisiae* encode divergent proteins. Mol Cell Biol 6:3711–3721.

Shan B, Medina JC, Santha E, Frankmoelle WP, Chou T-C, Learned RM, Narbut MR, Stott D, Wu P, Jaen JC, Rosen T, Timmermans PBMWM, Beckman H. 1999. Selective covalent modification of β-tubulin residue Cys-239 by T138067, an antitumor agent with in vitro efficacy against multidrug-resistant tumors. Proc Natl Acad Sci USA 96:5686–5691.

Sherman F, Hicks J. 1991. Micromanipulation and dissection of asci. Methods Enzymol 194:21–37.

Shivanna BD, Mejillano MR, Williams TD, Himes RH. 1993. Exchangeable GTP binding site of β-tubulin. J Biol Chem 268: 127–132.

Tirnauer JS, O'Toole E, Berrueta L, Bierer BE, Pellman D. 1999. Yeast Bim1p promotes the G1-specific dynamics of microtubules. J Cell Biol 145:993–1007.